Journal of Visualized Experiments

Using Real-Time Cell Metabolic Flux Analyzer to Monitor Osteoblast Bioenergetics

--Manuscript Draft--

Article Type:	Invited Results Article - JoVE Produced Video
Manuscript Number:	JoVE63142R2
Full Title:	Using Real-Time Cell Metabolic Flux Analyzer to Monitor Osteoblast Bioenergetics
Corresponding Author:	Elizabeth Rendina-Ruedy Vanderbilt University Medical Center Nashville, TN UNITED STATES
Corresponding Author's Institution:	Vanderbilt University Medical Center
Corresponding Author E-Mail:	elizabeth.rendina-ruedy@vumc.org
Order of Authors:	Elizabeth Rendina-Ruedy
	Shobana Jayapalan
	Ananya Nandy
Additional Information:	
Question	**Response**
Please specify the section of the submitted manuscript.	Biology
Please indicate whether this article will be Standard Access or Open Access.	Standard Access ($1400)
Please indicate the **city, state/province, and country** where this article will be **filmed**. Please do not use abbreviations.	Nashville, TN, United States of America
Please confirm that you have read and agree to the terms and conditions of the author license agreement that applies below:	I agree to the Author License Agreement
Please confirm that you have read and agree to the terms and conditions of the video release that applies below:	I agree to the Video Release
Please provide any comments to the journal here.	

TITLE:

Using Real-Time Cell Metabolic Flux Analyzer to Monitor Osteoblast Bioenergetics

AUTHORS AND AFFILIATIONS:

Shobana Jayapalan[1,2], Ananya Nandy[1,2], Elizabeth Rendina-Ruedy[1,2,3]

[1]Vanderbilt Center for Bone Biology, Division of Clinical Pharmacology, Vanderbilt University Medical Center, Nashville, TN 37232; USA

[2]Department of Medicine, Division of Clinical Pharmacology, Vanderbilt University Medical Center, Nashville, TN 37232; USA

[3]Department of Molecular Physiology and Biophysics, Vanderbilt University, Nashville, TN 37232; USA

Email addresses of co-authors:

Shobana Jayapalan (shobanajayapalan@gmail.com)

Ananya Nandy (ananya.nandy@vumc.org)

Elizabeth Rendina-Ruedy (elizabeth.rendina-ruedy@vumc.org)

Corresponding author:

Elizabeth Rendina-Ruedy (elizabeth.rendina-ruedy@vumc.org)

SUMMARY:

Real-time cell metabolic flux assay measures the oxygen consumption rate and extracellular acidification rate, which corresponds to mitochondrial and glycolytic adenosine triphosphate production, using pH and oxygen sensors. The manuscript explains a method to understand the energy status of osteoblasts and the characterization and interpretation of the cellular bioenergetic status.

ABSTRACT:

Bone formation by osteoblasts is an essential process for proper bone acquisition and bone turnover to maintain skeletal homeostasis, and ultimately, prevent fracture. In the interest to both optimize peak bone mass and combat various musculoskeletal diseases (i.e., post-menopausal osteoporosis, anorexia nervosa, type 1 and 2 diabetes mellitus), incredible efforts have been made in the field of bone biology to fully characterize osteoblasts throughout their differentiation process. Given the primary role of mature osteoblasts to secrete matrix proteins and mineralization vesicles, it has been noted that these processes take an incredible amount of cellular energy, or adenosine triphosphate (ATP). The overall cellular energy status is often referred to as cellular bioenergetics, and it includes a series of metabolic reactions that sense substrate availability to derive ATP to meet cellular needs. Therefore, the current method details the process of isolating primary, murine bone marrow stromal cells (BMSCs) and monitoring their bioenergetic status using the Real-time cell metabolic flux analyzer at various stages in osteoblast differentiation. Importantly, these data have demonstrated that the metabolic profile changes dramatically throughout osteoblast differentiation. Thus, using this physiologically relevant cell type is required to fully appreciate how a cell's bioenergetic status can regulate the overall

function.

INTRODUCTION:

The formation of bone by the osteoblast is accompanied by coordinated destruction or resorption of bones by osteoclasts. The balance between osteoblastic bone formation and osteoclast resorption is a coupled process describing bone turnover or remodeling, which is essential for skeletal homeostasis. Osteoblast dysfunction leads to impaired bone formation and results in various diseases, including osteoporosis[1–3]. *Ex vivo/in vitro* differentiation of bone marrow stromal stem cells (BMSCs) to osteoblast precursors and mature osteoblasts results in the formation and deposition of the mineralized bone matrix in the culture vessel over time[4–6]. This bone formation by the osteoblast requires a significant amount of cellular energy. Specifically, collagen synthesis and secretion have been shown to rely heavily on cellular ATP: ADP ratios, and presumably, mineralized vesicle trafficking and secretion require additional ATP[7–11]. Many researchers have demonstrated that the process of osteoblastogenesis and osteoblast function requires an adequate supply of energy to meet the metabolic demand of bone formation[12–16]. Therefore, the goal of this method is to characterize the bioenergetic status of primary, murine stromal cells throughout osteoblast differentiation using the real-time cell metabolic flux analyzer. These techniques aid in developing a better understanding of skeletal homeostasis, which may ultimately lead to the development of novel therapeutic options capable of improving skeletal-related outcomes.

The real-time cell metabolic flux analyzer can be used to measure the oxygen consumption rate (OCR) and extracellular acidification rate (ECAR) of live osteoblasts, which corresponds to mitochondrial and glycolytic ATP production, respectively. Fundamental to this methodology is the fact that one H^+ ion per lactate is released during glycolysis in the conversion of glucose to lactate, which alters media pH reflected in the ECAR values. Conversely, during the TCA (tricarboxylic acid) cycle, oxidative phosphorylation *via* the mitochondria produces CO_2 by utilizing or consuming oxygen, and therefore monitoring OCR is reflective of this metabolic process. The analyzer measures both OCR and ECAR in the extracellular microenvironment simultaneously and in real-time, which allows for tremendous potential when studying cellular bioenergetics[6,17]. Additionally, performing these assays is relatively straightforward and easily customizable depending on the experimental goal. Similar techniques have been employed to further understand T-cell metabolic regulation of the immune system[18,19], cancer initiation, and progression[20], along with multiple other cell types contributing to metabolic syndromes[21,22].

The advantages of Real-time metabolic flux analyzer over alternative techniques include (1) the capability to measure cellular bioenergetics of live cells in real-time, (2) ability to perform assay with a relatively small number of cells (requires as low as 5,000 cells), (3) injection ports to parallelly manipulate multiple treatments in a high-throughput 96-well system, (4) use of radioactive label-free automated cell imager for normalization[18,23,24]. The following methods aim to provide a generalized but detailed description of how to monitor cellular bioenergetics in murine BMSCs throughout osteoblast differentiation using the analyzer. It will include routinely performed assays; however, as with many techniques and methods, it is highly encouraged that individual labs determine specific details for their experiments.

Selection of assay and different types of assays available: A wide variety of assay kits and reagents are available to study the bioenergetics of cells while ensuring the reliability and consistency of the experimental results. Additionally, the desktop software also offers assay templates that can be easily customized. The assay can be defined based on the user's needs to measure different metabolic parameters. These assays can be modified in various ways based on the experimental goal and/or scientific question. For example, with four injection ports, multiple compounds can be injected into the assay media to analyze the cellular response specific to each metabolic pathway.

Cell energy phenotype test: This assay measures the live cells' metabolic phenotype and metabolic potential. This assay is also recommended as the first step to get a generalized idea of pathway-specific metabolism. A mixture of oligomycin A—an inhibitor of ATP synthase and Carbonyl cyanide 4-(trifluoromethoxy) phenylhydrazone (FCCP)—a mitochondrial uncoupling agent is injected to understand the cell energy potential. The injection of oligomycin A inhibits the synthesis of ATP, resulting in an increase in the rate of glycolysis (ECAR) to enable the cells to meet their energy demands; on the other hand, the injection of FCCP results in higher OCR due to depolarization of the mitochondrial membrane. Essentially, this assay depicts basal metabolic respiration, and following the dual injections, pushes, or stresses, the metabolic response. Based on these parameters, the software then plots OCR and ECAR of the cells by classifying the cells as aerobic, quiescent, glycolytic, or energetic state over time[25,26].

ATP real-time production rate assay: This measures the cellular ATP production simultaneously from glycolysis and mitochondrial respiration. This assay quantitatively measures the metabolic shifts from the two energy pathways and provides data on the mitochondrial and glycolytic ATP production rates over time. The assay obtains basal OCR and ECAR data followed by calculating mitochondrial ATP production rate through injection of oligomycin A and glycolytic ATP production rate through injection of rotenone + antimycin A mixture (total inhibition of mitochondrial function), resulting in mitochondrial acidification[17,27].

Cell mitochondria stress test (or cell mito stress test): This measures the mitochondrial function through ATP-linked respiration, quantifies cellular bioenergetics, identifies mitochondrial dysfunction, and measures cells' response to stress. Various parameters, including basal and spare respiratory capacity, ATP-linked respiration, maximal respiration, and non-mitochondrial oxygen consumption, can be obtained in one assay. This assay involves serial injections of oligomycin A, FCCP (mitochondrial uncoupling agent), rotenone/antimycin A mixture inhibitors to efficiently analyze the effect of these on the mitochondrial function[28].

Flexibility mito fuel flex test: This measures the mitochondrial respiration rate by the oxidation of the three primary mitochondrial fuels by the presence and absence of their inhibitors. The sequential inhibition of glucose, glutamine, and fatty acids aids in measuring the dependency, capacity, and flexibility of cells and the dependency of the cells in various cellular pathways to meet the energy demand. When the mitochondria cannot meet the demands of the blocked pathway of interest by oxidizing other fuels, the cells enter a dependency state. The capacity of the cells is calculated by inhibition of the other two alternative pathways followed by the

inhibition of the pathway of interest. The flexibility of cells helps in understanding the ability of mitochondria to compensate and meet the fuel needs of the inhibited pathway. It is calculated by subtracting the dependency of cells from the capacity of cells. Three different inhibitors are used independently or as a mixture of two to effectively calculate the assay parameters. 2-cyano-3-(1-phenyl-1H-indol-3-yl)-2-propenoic acid (UK5099) inhibits the oxidation of glucose by blocking the pyruvate carrier in glycolysis. Bis-2-(5-phenylacetamido-1,3,4-thiadiazol-2-yl) (BPTES) ethyl sulfide inhibits the glutamine oxidation pathway, and etomoxir inhibits the oxidation of long-chain fatty acids[29].

[Place **Figure 1** here]

PROTOCOL:

All the procedures were based on the guidelines and approval of the Institutional Animal Care and Use Committee at Vanderbilt University Medical center.

1. Preparation of reagents and assay setup

1.1. Isolation and culturing of bone marrow stromal cells (also see the previous article[30]).

1.1.1. Prepare complete alpha minimum essential media (αMEM) cell culture media by supplementing minimum essential media with alpha modification with 10% FBS (fetal bovine serum), 100 U/mL of penicillin, and 100 µg/mL of streptomycin.

1.1.2. Prepare the bone marrow collection tube by trimming the end of a 0.6 mL microcentrifuge tube so that the cells can pass through and inserting it in a 1.5 mL microcentrifuge tube containing 100 µL of complete αMEM.

1.1.3. Euthanize the mice using CO_2 treatment as follows. Place the animal in the CO_2 chamber for 2–3 min or until respiration ceases. Wait for at least 1 min after the animal becomes unconscious to remove the mice from the chamber and cervically dislocate.

1.1.4. Using sterile forceps and a pair of scissors, cut open the lower abdomen of the euthanized mice to make a small incision. Isolate the long bones (femur, tibia, and iliac crest) of the mice.

1.1.5. Trim the long bones to remove all soft tissue. Once the bone is cleaned, cut ~1–2 mm from the distal and proximal ends to create an opening for the marrow to flush through.

NOTE: This opening should be conservative so as not to lose the marrow while allowing it to flush out.

1.1.6. Place the bones in a collection tube containing 100 µL of 1x sterile PBS (phosphate-buffered saline) to isolate the total bone marrow.

1.1.7. Flush the marrow by centrifugation at 10,000 x *g* for 15–20 s at room temperature. Marrow cells pellet at the bottom of the tube.

1.1.8. Repeat centrifugation until the bone cavity appears white and devoid of most marrow elements. Resuspend the mixed population of bone marrow by gently pipetting up and down.

1.1.9. Culture the cells from one animal (both femur and tibia) in a 75 cm^2 cell culture flask in 10 mL of cell culture media and incubate at 37 °C in a cell culture incubator with 5% CO_2. If pooling cells from 2–3 animals, use a 150 cm^2 cell culture flask (recommended).

1.1.10. Following 24–48 h of incubation of the mixed population, aspirate the non-adherent hematopoietic cell population contained within the culture media and wash the adherent cells with 1x PBS.

1.2. Cell seeding from BMSCs and osteoblast differentiation

1.2.1. Trypsinize the adherent cells by adding enough 0.25% trypsin- EDTA (approximately 3–4 mL) to slightly cover the flask surface, followed by a 3 min incubation at 37 °C.

1.2.2. Add 6–7 mL of complete αMEM to the flask/trypsin to resuspend the adherent BMSCs by carefully pipetting up and down. Transfer BMSC suspension to a conical centrifuge tube.

1.2.3. Remove a 50 µL aliquot of the BMSC suspension and add 50 µL of trypan blue (1:1 dilution) to it. Count the total number of viable cells that exclude the dye by pipetting 10 µL of this mixture onto a hemocytometer and observing it under the microscope. Do not count any dead or unhealthy cells that appear blue-colored (<10% cells).

1.2.4. Based on the cell count, calculate the volume of cell suspension in complete αMEM needed for a final concentration of 2.4 x 10^6 cells/mL for a total volume of at least 10 mL per plate.

[Place **Figure 2** here]

1.2.5. Centrifuge the cells in the conical tube at 1,000 x *g* for 5 min and resuspend the cells to the desired final concentration of 2.4 x 10^6 cells/mL.

1.2.6. Transfer the cell suspension to a reservoir and, using a multichannel pipet, carefully resuspend the cells to ensure a homogenous mixture of cells.

1.2.7. Seed 2.5 x 10^4 cells per well in the 96-well cell culture microplate with 80 µL of complete αMEM. Do not seed cells in the background correction wells (A1, A12, H1, H12); instead, just add the medium in these four wells.

NOTE: BMSCs for the assays are plated in 96-well cell culture microplate designed for the analyzer

in conjunction with the sensor cartridges. The surface area of these plates is different from a regular 96-well plate. The surface area of each well in the plate is 0.106 cm^2, which is approximately 40% of the typical 96-well plate area. Optimal cell seeding density is chosen based on the cell type. Typically, the analyzer can detect between 0.5–4 x 10^4 cells per well. Osteoblasts need to be in contact to differentiate effectively; for this purpose, plating between 2.0 x 10^4–3.0 x 10^4 BMSCs/well in 80 µL of complete αMEM has been selected.

1.2.8. Gently agitate the plate to ensure the even distribution of cells in the wells and incubate at 37 °C, 5% CO_2. Check the growth of the cells and cell confluency under the microscope after 48 h. Change the cell culture media if required.

1.2.9. Depending on the goal of the assay, when BMSCs are 60%–80% confluent (typically 48–72 h), initiate osteoblast differentiation by changing the cell culture media to osteoblast differentiation media (complete αMEM supplemented with 5 mM β-glycerol phosphate and 50 µg/mL of L-ascorbic acid).

1.2.10. If undifferentiated stromal cells (Day 0) are to be analyzed, maintain cells under complete αMEM.

1.2.11. Change the osteoblast differentiation media every other day and visualize the cells under the microscope to ensure they are healthy until the day of the assay. Preferably, 24 h before the scheduled assay, change the media and maintain a consistent medium change schedule (recommended).

NOTE: Carefully change the media by slightly tilting the plates at an angle; this avoids accidental contact of pipette tips to the cell culture plates and disruption of the monolayer of cells.

2. Preparation of sensor cartridge for extracellular flux calibration

2.1. Hydrate the sensor cartridges from the extracellular assay kit prior to the day of the assay. Remove the sensor cartridges (green plate) and place the sensors upside down.

2.2. Using a multichannel pipet, add 200 µL of H_2O to each well of the utility plate. Carefully place the sensor cartridges back on the utility plate and incubate the plate overnight at room temperature.

NOTE: The manufacturer recommends incubating the sensor cartridges in a non-CO_2 37 °C incubator overnight. However, significant evaporation of the sensor cartridges can occur. If this happens, sensor cartridges can be incubated at room temperature. These plates should be incubated for a minimum of 4 h and a maximum of 72 h.

2.3. On the day of the assay, discard the H_2O from the utility plate and add 200 µL of calibrant. Incubate the utility plate for at least 1 h before the assay.

3. Real-time cell metabolic flux analyzer media preparation

3.1. Use the DMEM media with a pre-adjusted pH of 7.4 (recommended) to run the assay with BMSCs.

3.2. Prepare 80 mL of assay media by supplementing DMEM media with 1 mM sodium pyruvate, 2 mM glutamine, 10 mM glucose, 200 nM insulin, 50–200 µM oleic acid BSA.

3.3. Incubate the complete assay media at 37 °C in a water bath.

4. Preparation of compounds for the sensor cartridges

4.1. Thaw oligomycin A, rotenone, and antimycin A on ice. Pipette up and down to solubilize the compounds before use.

4.2. Add 3 mL of prepared assay medium to each tube, followed by the addition of the respective compound—tube A: 26.4 µL of 2.5 mM oligomycin A; tube B: 3.1 µL of 12.67 mM rotenone + 4.1 µL of 9.4 mM antimycin A + 30 µL Hoechst stain.

4.3. Load a 10x concentration of these inhibitors in the corresponding port. The final concentration of injection solutions needed is 2 µM of oligomycin A, 1 µM of rotenone, and 4.1 µM of antimycin A.

NOTE: Hoechst is added to the final injection port for fluorescently staining the nuclei for imaging and normalization purposes. These concentrations can be optimized based on the cell type.

4.4. Load 20 µL of these compounds into the cells in 180 µL of assay media.

5. Prepare cell culture microplate for assay

5.1. Remove the cell culture microplate from the 37 °C incubator and observe the cells under the microscope.

5.2. Remove the assay medium from the water bath.

5.3. Gently wash the cells with 200 µL of assay medium twice and add 200 µL of assay media per well.

NOTE: Once the final assay media is added to the cells, the time until the plates get into the analyzer is crucial. Therefore, do not begin replacing the media until the following steps are performed within 1 h.

5.4. Check the cells under the microscope to ensure that the cells remain adhered to the wells.

5.5. Ensure cells in D5 and E8 are adhered with a consistent monolayer and were not washed away during the washing step. Cell imaging software uses these two wells for setting the autofocus and autoexposure.

NOTE: The manufacturer recommends incubating the plate in a non-CO_2 37 °C incubator for 1 h; this step can be skipped if automated imaging is preferred. For example, the microplate imager maintains the same conditions in a closed chamber, and cells can be imaged under a brightfield.

6. Setting up the assay and imaging

[Place **Figure 3** here]

6.1. Open the desktop software in the computer next to the equipment.

6.2. Check the connection status in the lower-left corner of the controller software.

6.3. Go to **Templates** and select the **XF ATP Rate Assay** template file or appropriate assay template.

6.4. Select **Group Definitions** on the top of the screen and define the groups.

6.5. Select the **Plate Map Layout** and assign the wells depending on the groups defined.

6.6. Verify the instrument protocol, ensure that the compounds added are correctly listed, and include the project information for future references.

6.7. Click on **Run Assay**; this will prompt the selection of the result file storage location.

6.8. Select the location to save the result file.

6.9. Save the file with the date of assay and click on **Start Run.**

6.10. Place the sensor cartridge and the utility plate on the tray and click on **I'm Ready** to initiate the calibration.

6.11. Before starting the calibration**,** ensure the cartridge lid is removed, and the sensor cartridge is placed in the correct orientation on the utility plate. This step will take 10–20 min, and once complete, the software will display the **Load Cell Plate** dialog box.

7. Obtain brightfield images

NOTE: This step is optional. If no imaging equipment is available, skip to step 8.

[Place **Figure 4** here]

7.1. Open the cell imaging software on the computer.

7.2. Make sure that the microplate imager is turned on and the ports are connected to the computer.

7.3. Check the status bar in the bottom left of the screen to ensure that the temperature is set to 37 °C and that the connection status should be highlighted in green as ready.

7.4. Scan the plate barcode to initiate the imaging process.

7.5. Provide a name to the cell plate and hit **Save** (This is the name where both bright field and fluorescent images will be saved). Click on **Perform Brightfield Scan**.

7.6. The next screen, plate, and scan menu, show the options for imaging. Before the assay, select **Start Brightfield Scan**.

7.7. Place the cell culture microplate along with the plate cover/lid on the tray holder and align well A1 with the A1 Mark. Click on **Close Tray**.

7.8. The next screen, brightfield image acquisition, with a plate map appears. Click on **Scan All Wells**, which initiates the system initialization process followed by 30 to 35 min of a scan.

7.9. After the brightfield scan, remove the cell culture microplate and place it in the analyzer to perform the assay.

8. Running the assay

8.1. Once the calibration is completed, the software displays the **Load Cell Plate** dialog box.

8.2. Click on **Open Tray** to replace the utility tray with a cell culture microplate. Ensure that the lid is removed and the A1 of the plate fits in the correct orientation.

8.3. Then, click on **Load Cell Plate** to initiate the assay. The sensor cartridge will remain inside the analyzer for the assay injections.

8.4. Wait until the assay starts and displays the estimated time of completion.

8.5. Upon completion of assay, the software displays **Unload Sensor Cartridge** dialog box. Click on **Eject** and remove the cell culture microplate from the analyzer.

8.6. Carefully remove the sensor cartridge and replace the cell plate lid. The cells are ready for fluorescent imaging and cell counting.

8.7. After removing the cell plate and sensor cartridge, the **Assay Complete** dialog box appears.

8.8. Click on **View Results** to open the assay result file and normalize the data immediately or click on **Home**.

9. Obtain fluorescence images and normalize

NOTE: This step is an optional but preferred method for the normalization of BMSCs and osteoblasts. If no imaging equipment is available, another normalization method needs to be performed, such as protein or DNA isolation and quantification.

[Place **Figure 5** here]

9.1. After the assay completion, scan the plate barcode with the handheld barcode reader. If the plate has already been imaged, it will not require a new name.

9.2. Select **Fluorescence & Cell Count**, place the cell plate on the tray holder, and click on **Close Tray**.

9.3. In the image acquisition window, select **Scan All Wells** to begin imaging. Fluorescence imaging takes about 15–20 min to scan the entire plate. Observe the green tick mark denoting that the scan has been completed.

9.4. Review the fluorescent images and cell counts in the imaging and cell imaging application by randomly clicking on a couple of the wells.

NOTE: There is an option to view counted cells on the bottom right of the screen. This option shows a masked image, highlighting the objects that were counted.

9.5. Once the fluorescence imaging is complete, export the images for additional references.

9.6. Once the imaging and cell count is complete, open the **Results** file and click on **Normalize**. The normalization screen will give the plate layout and an option to import the cell count.

9.7. Click on **Import** and select **Apply** for the desktop software to normalize the assay with cell count automatically.

REPRESENTATIVE RESULTS:

[Place **Figure 6** here]

The protocol describes a generalized description of how the extracellular flux assays aids in understanding the cellular bioenergetics of osteoblasts derived from murine BMSCs. We have

detailed these routinely performed assays and important notes to be considered before, during, and after the assay. The two major ATP production pathways, glycolysis, and mitochondrial oxidative phosphorylation, are widely discussed to better understand the capability of cells to interchange between the pathways, thereby meeting the energy demands of the cells. Once the assay is complete, the assay results are normalized based on the cell count and exported to the respective assay report generator file. The report generator automatically calculates the assay parameters and provides a summary report of the assay. **Figure 6** illustrates the representative results of routinely performed assays to better understand how mature osteoblasts control versus treatment groups react when different inhibitors are injected.

Generic, representative images of possible expected results are shown in **Figure 6**. For example, in **Figure 6A**, the cell energy phenotype monitors the OCR vs. ECAR by calculating the cells' baseline phenotype, stressed phenotype, and metabolic potential. The injection of the oligomycin A and FCCP stressor mix increases the control group's baseline activity (open symbols) by increasing the utilization of both pathways. In response to the stressors, a significantly high energy level is noticed in the control and treatment 1 group (closed symbols). On the other hand, treatment 2 had a comparatively lower baseline activity, and the cells became more aerobic. This assay aids in understanding the bioenergetics of the cells in response to different stressors.

Real-time ATP rate assay calculates the total cellular ATP production rate based on the sum of glycolytic and mitochondrial ATP production rates.

ATP Production Rate (pmol ATP/min) = glycoATP Production Rate (pmol ATP/min) + mitoATP Production Rate (pmol ATP/min).

Figure 6B indicates that both the control and treatment groups produce more ATP through glycolysis compared to that of oxidative phosphorylation. While the treatment group exhibits significantly higher total ATP production, the cells have consistently shifted from glycolytic to oxidative metabolism. This comparison of the control and treatment group indicates that this specific treatment exhibits a different bioenergetic profile compared to the control group.

Figure 6C is an example of the mitochondrial respiration rate over time, which is detailed. The basal respiration rate in the treatment group is comparatively less than in the control group. The respiration and ATP production rates in both groups are decreased along with the proton leak followed by an oligomycin A injection. The respiration rates of the cells rise back again to their maximal respiration after the injection of FCCP. The final injection of rotenone/antimycin A decreases the OCR again, resulting in spare respiration, which is measured by the differences in maximal and basal respiration. After the third injection, the mitochondrial respiration is shut down by the combination of rotenone/antimycin A, which targets and inhibits the electron transport chain (ETC) complex I and III, thereby enabling us to calculate the non-mitochondrial respiration. Compared to the control group, both the basal and maximal respiration in the treatment groups is relatively lower; this suggests that the treatment could affect the mitochondrial respiration of osteoblasts.

The mito fuel flex test measures the potential of mitochondria to oxidize the three different mitochondrial fuels, glucose, glutamine, and fatty acids. The cell's dependency, flexibility, and capacity on different pathways that fuel the mitochondrial respiration are calculated based on the oxidation of the respective mitochondrial fuel. **Figure 6D** shows that the control group is highly dependent on the glucose pathway. At the same time, the treatment enhanced the capacity of glucose oxidation of the cells to meet the fuel needs of the inhibited pathway actively. On the other hand, the oxidation of glutamine was efficient in the control group, resulting in comparatively higher dependency of cells to that of the treatment group, thereby increasing the overall capacity of the control group. The fatty acid pathway shows that the treatment has increased the overall capacity of the cells due to the higher dependency on mitochondrial fuel while compensating the fuel needs.

FIGURE AND TABLE LEGENDS:

Figure 1: Schematic representation of the methodology for culturing and preparing osteoblasts for analysis. Murine BMSCs are isolated from long bones, cultured, and seeded in 96-well plates at 25,000 cells/well density. When the cells are 80%–100% confluent, the cells are differentiated with osteoblast-specific media. The assays are performed at different stages of differentiation. The cartridge plates are hydrated 1 day prior to the assay. On the day of assay, different inhibitors are injected in the ports of the sensor cartridges based on the assay requirements, and a calibration buffer is added to the 96-well calibration plate. After calibration, the real-time cell metabolic flux assay is performed, followed by imaging the cell culture microplate using the microplate imager to normalize real-time cell metabolic flux analyzer data with cell count.

Figure 2: The cell culture microplate, specifically designed for the analyzer. (**A**) The four background correction wells, A1, A12, H1, H12, are highlighted. These wells only contain assay media without any cells. (**B**) The barcode on the side of the plate to scan the plate using the imaging reader and analyzer.

Figure 3: The controller software. To verify the equipment is connected and is set to 37 °C. The template files for different assays that can be performed with the extracellular flux analyzer can be selected to customize the assay further based on the experimental goals.

Figure 4: The cell imaging software communicates to the imaging reader through the computer. The cells in the microplate can be imaged before and after the assay, and the cell count/well is obtained after the assay to normalize the data.

Figure 5: Representative images from the imaging software used for normalization of data from the assay. (**A**) Stitched bright field image showing the cell confluence throughout the entire well. (**B**) Stitched fluorescence image showing Hoechst-stained nuclei of osteoblasts used for counting cell numbers to normalize the assay results. These are osteoblasts after 7 days of differentiation.

Figure 6: Representative graphs for routinely performed assay to understand the cellular bioenergetic profile of control vs. treatment group with their respective standard errors. (**A**) The cell energy phenotype test. The plot represents the glycolysis (ECAR) vs. mitochondrial respiration (OCR) of the control vs. two treatment groups (n = 3). The injection of oligomycin A

and FCCP stressors elevates the baseline activity, indicated by open symbols, and closed symbols indicate the response of cells to different stressors. (**B**) The real-time ATP rate assay. The ATP rate assay indicates that both the control and treatment groups (n = 2) produce more ATP through glycolysis compared to that of oxidative phosphorylation. (**C**) The mito stress test. The mito stress test provides the mitochondrial respiration rate of control vs. treatment cells (n = 2) over time and the effect of inhibitors on the cells after their respective injections. (**D**) The mito fuel flex test. The mito fuel flex test measures the percentage oxidation of control and treatment groups (n = 2) with respect to glucose, glutamine, and fatty acid pathways and the dependency and flexibility of the cells on these mitochondrial fuels.

DISCUSSION:

The real-time cell metabolic flux analyzer can be used to explore cellular energetics under different conditions. The protocol illustrates the efficient isolation of BMSCs, culturing cells in appropriate cell culture plates, and their differentiation to mature osteoblasts, which can be used for various assays using the extracellular flux analyzer. Further, the critical steps of real-time cell metabolic flux assay, including hydration of sensor cartridges, loading of the injection ports, performing the assay, normalization of the data, and data analyses, are also explained in detail. This assay evaluates the response of osteoblasts to different mitochondrial and glycolytic inhibitors to understand the bioenergetics of the cells. This protocol is optimized specifically for osteoblasts based on the cell type, and this method offers a more robust and precise guide compared to the manufacturer's standard protocol. Several parameters in this protocol, including the cell seeding density, the concentration of the compounds, addition of exogenous substrate to the media, buffering capacity, need to be optimized based on the specific cell type and its background.

The extracellular flux analyzer provides quick and reliable measures of cellular metabolic functions in *ex vivo* cultured cells. Compared to other biological assays, the total assay time is typically between 60 to 120 min. The equipment maintains normal cellular and physiological conditions by maintaining the preset temperature of 37 °C, facilitating efficient and reproducible assay results with reduced complexities. Typically, baseline OCR and ECAR are recorded three to four times before adding inhibitors. The inhibitors and treatments are also sequentially injected, facilitating the cell's metabolic response measurement over time. The analyzer allows researchers to achieve standardized results under optimized conditions. The analyzer also offers the ability to inject different compounds during the assay to observe real-time changes in the respiration of cells. For example, for ATP rate assay, use a 2 µM oligomycin A and 1 µM rotenone/1 µM antimycin A mixture as the default compound injected—Port A: 2 µM Oligomycin A; Port B: 1 µM Rotenone/1 µM Antimycin A.

The assay media is different from the typical growth media by a few factors, including the absence of bicarbonate to better detect changes in pH, the absence of glucose, glutamine, and pyruvate supplements allows the experimenter to customize the exogenous substrates added, and the media does not contain phenol red to precisely calculate the pH values.

Glucose, L-glutamine, and sodium pyruvate are the most used exogenous substrates. The use of

these substrates is specific to cell type and experimental questions. In this context, it is recognized that these assays, while valuable, are performed using an artificial system. For example, it is recommended to use 10 mM glucose; however, this is supraphysiological levels, and researchers should consider whether other glucose concentrations would be more appropriate. To this point, it is also essential to consider whether glucose uptake in BMSCs and osteoblasts depends on insulin, and in that case, insulin should also be added. Since this remains a topic of debate within the field[31,32], the inclusion of insulin is preferred. Along a similar line, if fatty acid utilization is relative to the experimental question, the assay media should be further supplemented with fatty acids. The importance of these exogenous substrates plays a critical role in the assays and data interpretation; therefore, concentrations of these substrates should be optimized based on the cell type and research question.

One of the primary advantages of the extracellular flux analyzer is that it requires a minimal number of cells to run the assays, with a high *n* given the 96-well format. The sensor cartridges also enable the ability to inject different inhibitors and compounds through the four injection ports. The flexibility to modify the assay, to perform acute injections with additional inhibitors and treatments of interest is an added advantage of this technique. These features make the analyzer capable of doing high throughput, real-time assays on a minimal number of cells and hence preferable over the classical Clark oxygen electrode method. Although the electrode method is inexpensive and simple for measuring mitochondrial respiration, it gives far higher background noise and has a lower resolution than the analyzer[24,33].

Additionally, in the workflow described, the cell bioenergetic profile obtained from the analyzer can efficiently be normalized using the microplate imager by counting the cells in the microplates after the assay[34]. The number of viable cells may vary from well to well after the assay; use of cell count is preferable over other methods, including the protein or DNA normalization as the protein or DNA content of cells does not remain constant under different conditions or treatments for which the cellular energetics are being compared. The protein or DNA content may vary under the influence of different treatments and is a major disadvantage of normalization using this method. For example, the protein content of osteoblast changes during differentiation. As the cells mature during osteoblastogenesis, they start secreting extracellular matrix protein increasing the total cellular protein content. This can be problematic when comparing the assay results of cells under different growth phases or time points of osteoblastogenesis.

Given the multitude of advantages, the analyzer to monitor cellular bioenergetics has been a tremendous addition to advancing the field. However, limitations do exist. For example, one of the major limitations of these assays is that they can only be performed at the cellular or organoid level, and the data is not sufficient to provide us with a complete idea of what would happen *in vivo* under different physiological conditions. As mentioned previously, the cellular environment created during the assays is also far from the original physiological niche. The artificial micro-environment created by supplementing different nutrients like glucose, pyruvate, glutamine, and oleic or palmitic acid are often higher than the normal physiological levels of the osteoblasts. The addition of fatty acid as one of the nutrients for the assay is limited, as most of the higher carbon

chain length fatty acids present in our body are very hydrophobic and highly insoluble. This results in technical difficulties in adding them to the assay media. The metabolic response of cells to single fatty acid like oleic or palmitic acid is different under other physiological conditions, where the cells experience a cocktail of various fatty acids and binding proteins. Finally, the measurement of ATP using this method, while arguably superior to static luminescent assays, remains indirect as this technique only measures oxygen. While it is not a direct measurement, it is true that the addition of the ATP synthase inhibitor, oligomycin A, followed by electron transport chain inhibitors while measuring OCR provides strong evidence of changes occurring in ATP. Therefore, techniques like mass spectroscopy can be used to support these data. Nonetheless, while these limitations should be carefully considered, this tool provides invaluable information relative to cellular bioenergetics.

Finally, it is noted that to understand how the said alterations in bioenergetics impact cellular functionality, specifically of the BMSCs and osteoblasts, complementary experiments are needed to be included *in vitro* culturing followed by alkaline phosphatase (ALIP), Von Kossa, or Alizarin staining.

In conclusion, the methods described above provide the basis for monitoring various metabolic pathways in osteoblasts using the real-time cell metabolic flux analyzer. Performing such experiments will lead to a deeper understanding of how cellular bioenergetics in primary, murine BMSCs throughout osteoblast differentiation can be modulated to improve skeletal-related outcomes.

ACKNOWLEDGMENTS:

This work was supported by the National Institute of Health (NIH) National Institute of Arthritis and Musculoskeletal and Skin Diseases (NIAMS) Grant AR072123 and National Institute on Aging (NIA) Grant AG069795 (to ERR).

DISCLOSURES:

The authors have nothing to disclose.

REFERENCES:

1. Rodan, G. A. Bone homeostasis. *Proceedings of the National Academy of Sciences of the United States of America*. **95** (23), 13361–13362 (1998).
2. Nakahama, K. I. Cellular communications in bone homeostasis and repair. *Cellular and Molecular Life Sciences*. **67** (23), 4001–4009 (2010).
3. Kim, J. M., Lin, C., Stavre, Z., Greenblatt, M. B., Shim, J. H. Osteoblast-osteoclast communication and bone homeostasis. *Cells*. **9** (9), 2073 (2020).
4. Gao, J. et al. SIRT3/SOD2 maintains osteoblast differentiation and bone formation by regulating mitochondrial stress. *Cell Death and Differentiation*. **25** (2), 229–240 (2018).
5. Baron, R. Molecular mechanisms of bone resorption by the osteoclast. *The Anatomical Record*. **224** (2), 317–324 (1989).
6. Tian, L., Rosen, C. J., Guntur, A. R. Mitochondrial Function and Metabolism of Cultured Skeletal Cells. *Methods in Molecular Biology (Clifton, N.J.)*. **2230**, 437–447 (2021).

7. Zanotelli, M. R. et al. Regulation of ATP utilization during metastatic cell migration by collagen architecture. *Molecular Biology of the Cell*. **29** (1), 1–9 (2018).
8. Gonzales, S., Wang, C., Levene, H., Cheung, H. S., Huang, C. Y. C. ATP promotes extracellular matrix biosynthesis of intervertebral disc cells. *Cell and Tissue Research*. **359** (2), 635–642 (2015).
9. Kruse, N. J., Bornstein, P. The metabolic requirements for transcellular movement and secretion of collagen. *Journal of Biological Chemistry*. **250** (13), 4841–4847 (1975).
10. Rendina-Ruedy, E., Guntur, A. R., Rosen, C. J. Intracellular lipid droplets support osteoblast function. *Adipocyte*. **6** (3), 250–258 (2017).
11. Sinnott-Armstrong, N. et al. A regulatory variant at 3q21.1 confers an increased pleiotropic risk for hyperglycemia and altered bone mineral density. *Cell Metabolism*. **33** (3), 615–628.e13 (2021).
12. Esen, E., Lee, S. Y., Wice, B. M., Long, F. PTH promotes bone anabolism by stimulating aerobic glycolysis via IGF signaling. *Journal of Bone and Mineral Research*. **30** (11), 1959–1968 (2015).
13. Borle, A. B., Nichols, N., Nichols, G. Metabolic studies of bone in vitro: I. Normal bone. *Journal of Biological Chemistry*. **235**, 1206–1210 (1960).
14. Borle, A. B., Nichols, N., Nichols, G. Metabolic studies of bone in vitro: II. The metabolic patterns of accretion and resorption. *Journal of Biological Chemistry*. **235**, 1211–1214 (1960).
15. Adamek, G., Felix, R., Guenther, H. L., Fleisch, H. Fatty acid oxidation in bone tissue and bone cells in culture. Characterization and hormonal influences. *The Biochemical Journal*. **248** (1), 129–137 (1987).
16. Frey, J. L. et al. Wnt-Lrp5 signaling regulates fatty acid metabolism in the osteoblast. *Molecular and Cellular Biology*. **35** (11), 1979–1991 (2015).
17. Romero, N., Rogers, G., Neilson, A., Dranka, B. P. Quantifying cellular ATP production rate using agilent seahorse XF technology (2018).
18. van der Windt, G., Chang, C., Pearce, E. Measuring bioenergetics in T cells using a Seahorse Extracellular Flux Analyzer. *Current Protocols in Immunology*. **113**:3.16B.1–3.16B.14. (2016).
19. Traba, J., Miozzo, P., Akkaya, B., Pierce, S. K., Akkaya, M. An optimized protocol to analyze glycolysis and mitochondrial respiration in lymphocytes. *Journal of Visualized Experiments: JoVE*. (117), 54918 (2016).
20. Noel, P. et al. Preparation and metabolic assay of 3-dimensional spheroid co-cultures of pancreatic cancer cells and fibroblasts. *Journal of Visualized Experiments: JoVE*. (126), 56081 (2017).
21. Nicholls, D. et al. Bioenergetic profile experiment using C2C12 myoblast cells. *Journal of Visualized Experiments: JoVE*. (46), 2511 (2010).
22. Sakamuri, S. S. V. P. et al. Measurement of respiratory function in isolated cardiac mitochondria using Seahorse XFe24 Analyzer: applications for aging research. *GeroScience*. **40** (3), 347–356 (2018).
23. What are the advantages of using Seahorse XF technology? at <https://www.agilent.com/en/support/cell-analysis/advantages-of-using-xf-tech>.
24. Horan, M. P., Pichaud, N., Ballard, J. W. O. Review: Quantifying mitochondrial dysfunction

in complex diseases of aging. *Journals of Gerontology - Series A Biological Sciences and Medical Sciences*. **67 A** (10), 1022–1035 (2012).
25. XF cell energy phenotype test. at <https://www.agilent.com/en/product/cell-analysis/real-time-cell-metabolic-analysis/xf-assay-kits-reagents-cell-assay-media/seahorse-xf-cell-energy-phenotype-test-kit-740884>.
26. Leung, D. T. H., Chu, S. Measurement of oxidative stress: Mitochondrial function using the seahorse system. *Methods in Molecular Biology (Clifton, N.J.)*. 1710, 285–293 (2018).
27. XF ATP rate assay. at <https://www.agilent.com/en/product/cell-analysis/real-time-cell-metabolic-analysis/xf-assay-kits-reagents-cell-assay-media/seahorse-xf-real-time-atp-rate-assay-kit-740889>.
28. XF cell mito stress test. at <https://www.agilent.com/en/product/cell-analysis/real-time-cell-metabolic-analysis/xf-assay-kits-reagents-cell-assay-media/seahorse-xf-cell-mito-stress-test-kit-740885>.
29. XF mito fuel flex test. at <https://www.agilent.com/en/product/cell-analysis/real-time-cell-metabolic-analysis/xf-assay-kits-reagents-cell-assay-media/seahorse-xf-mito-fuel-flex-test-kit-740888>.
30. Maridas, D. E., Rendina-Ruedy, E., Le, P. T., Rosen, C. J. Isolation, culture, and differentiation of bone marrow stromal cells and osteoclast progenitors from mice. *Journal of Visualized Experiments: JoVE*. (131), 56750 (2018).
31. Wei, J. et al. Glucose uptake and Runx2 synergize to orchestrate osteoblast differentiation and bone formation. *Cell*. **161** (7), 1576–1591 (2015).
32. Zoch, M. L., Abou, D. S., Clemens, T. L., Thorek, D. L. J., Riddle, R. C. In vivo radiometric analysis of glucose uptake and distribution in mouse bone. *Bone Research*. **4**, 16004 (2016).
33. Divakaruni, A. S., Paradyse, A., Ferrick, D. A., Murphy, A. N., Jastroch, M. Analysis and interpretation of microplate-based oxygen consumption and pH data. *Methods in Enzymology*. **547** (C), 309–354 (2014).
34. Kam, Y., Jastromb, N., Clayton, J., Held, P., Dranka, B. Normalization of agilent seahorse XF data by in-situ cell counting using a BioTek cytation 5 application note (2017).

Figure 1

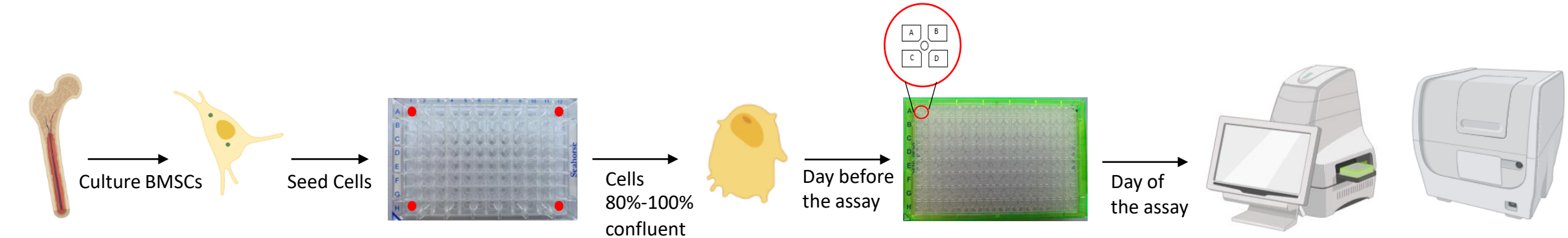

Figure 2

Click here to access/download;Figure;Figure 2.pdf

A.

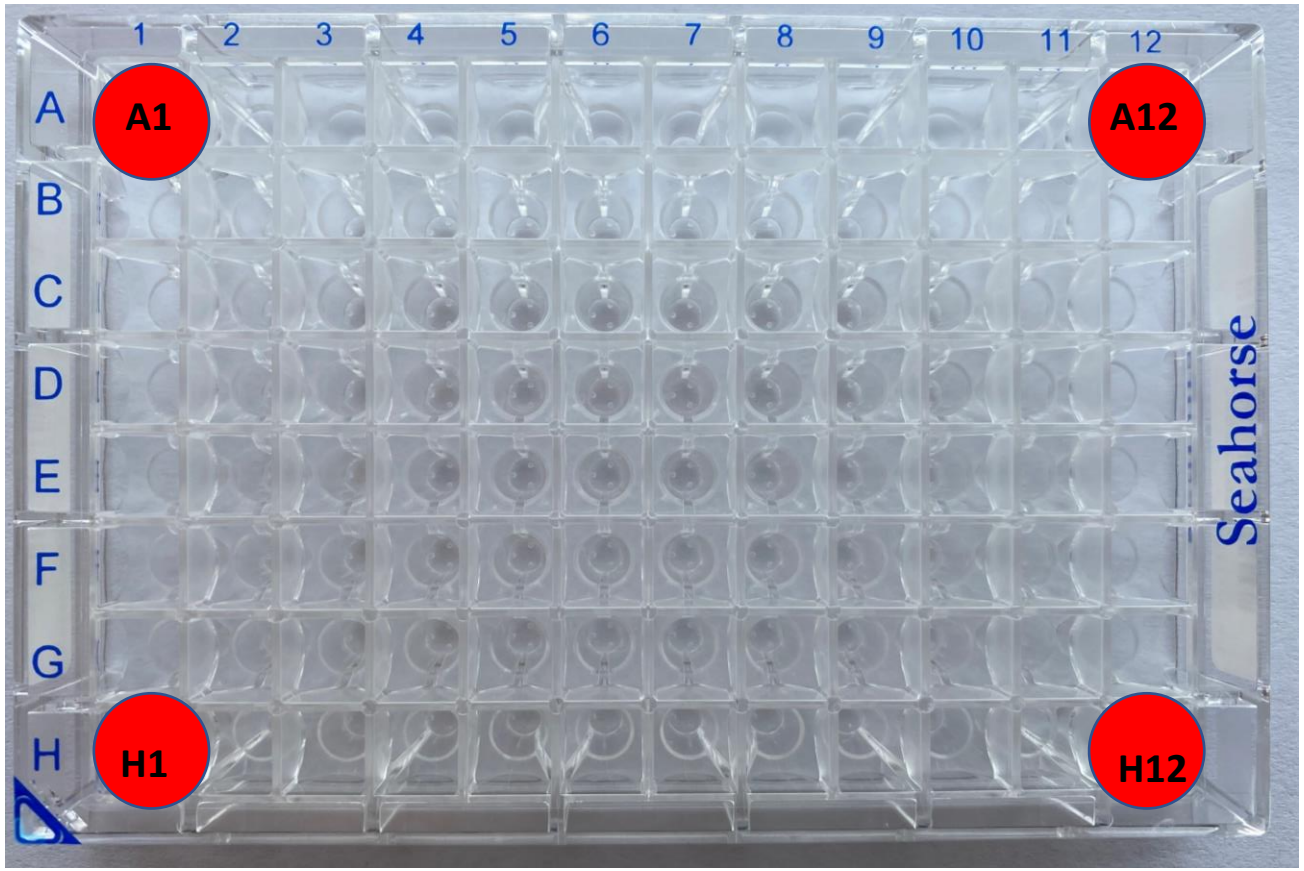

B.

Figure 3

Click here to access/download;Figure;Figure 3.pdf

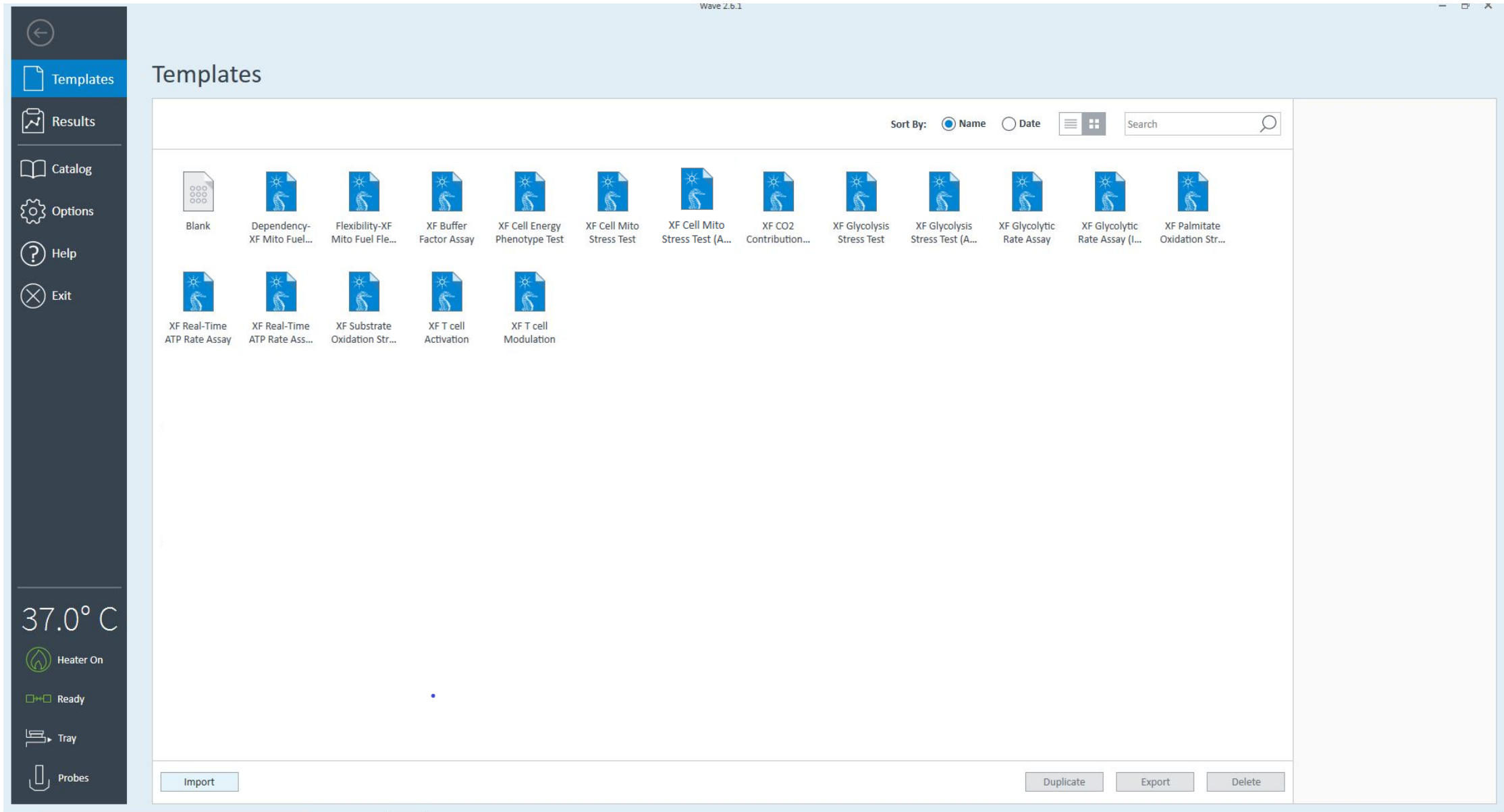

Figure 4

Click here to access/download;Figure;Figure 4_Updated.pdf

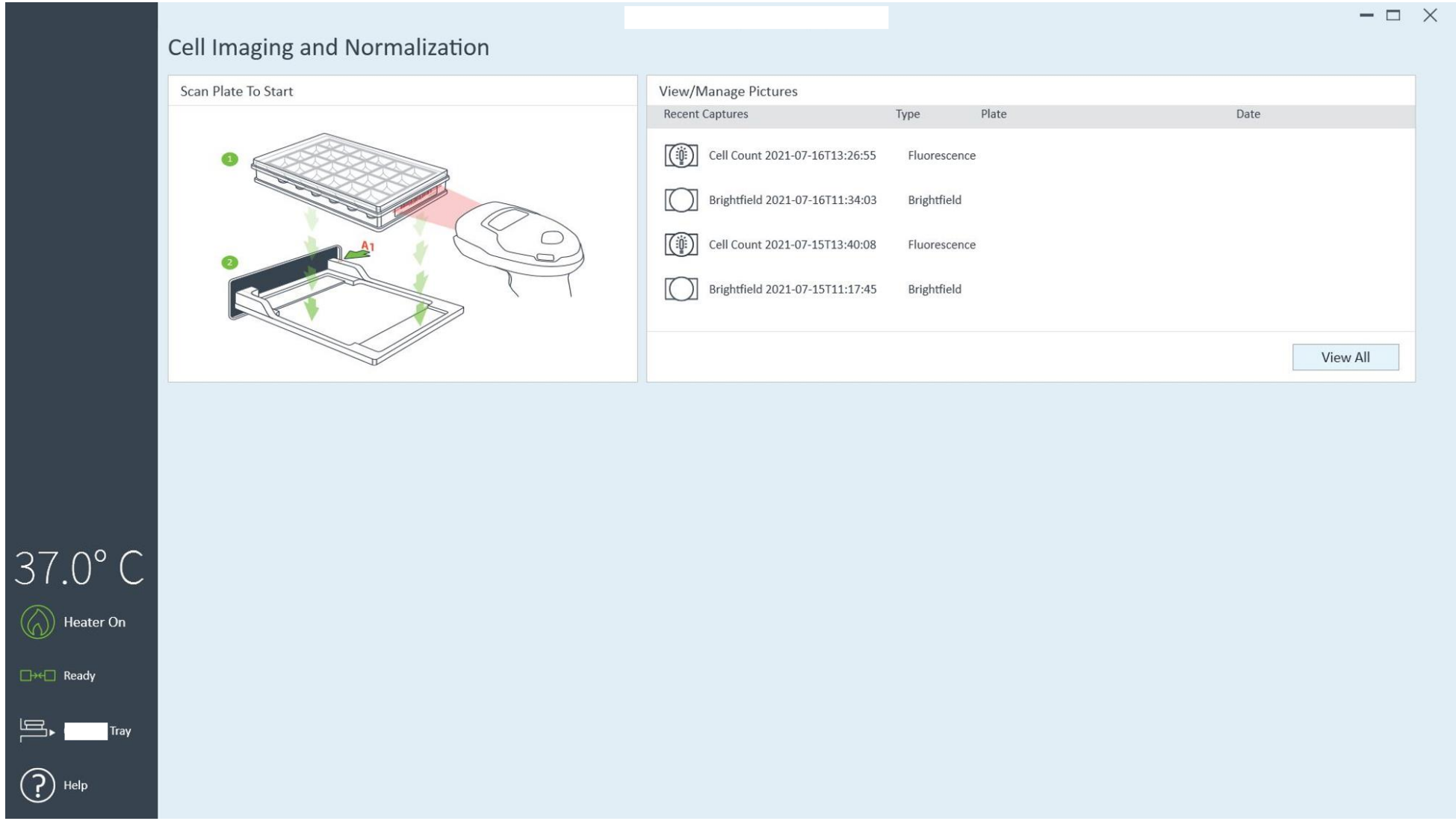

Figure 5

A.

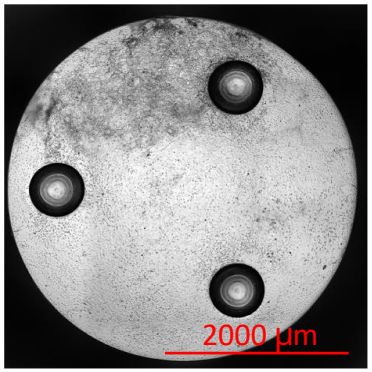

B.

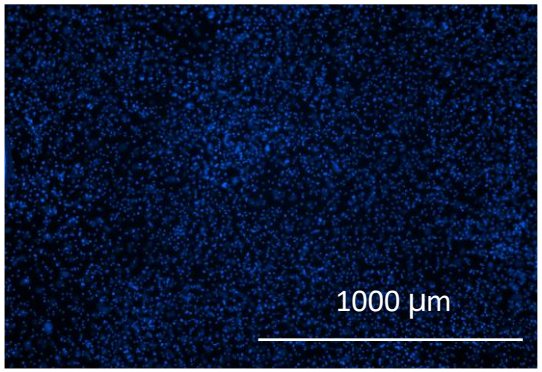

Figure 6

A.

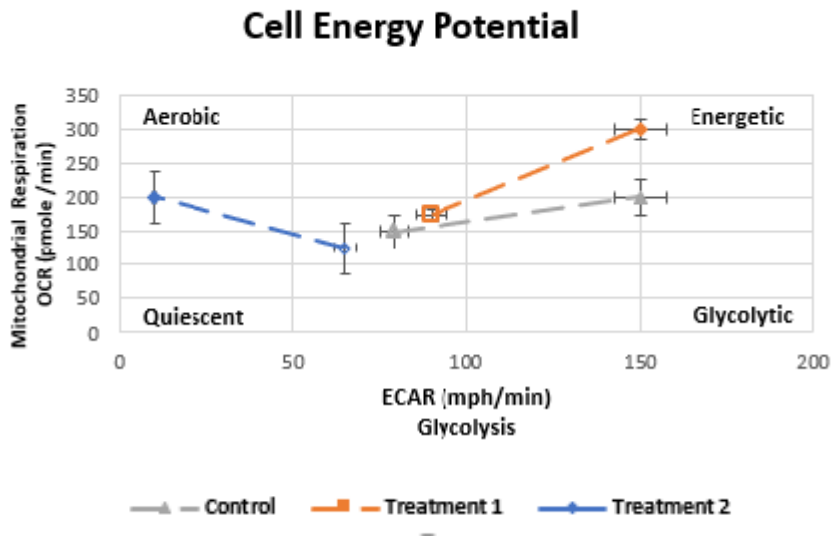

B.

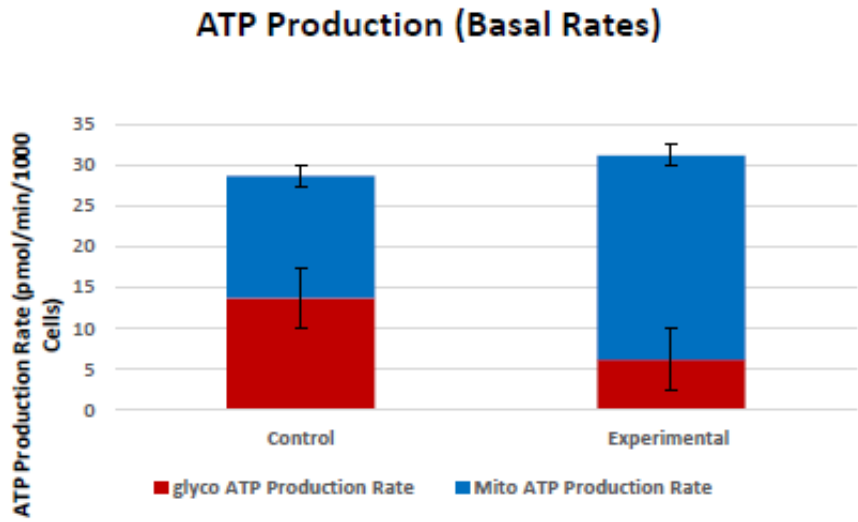

C.

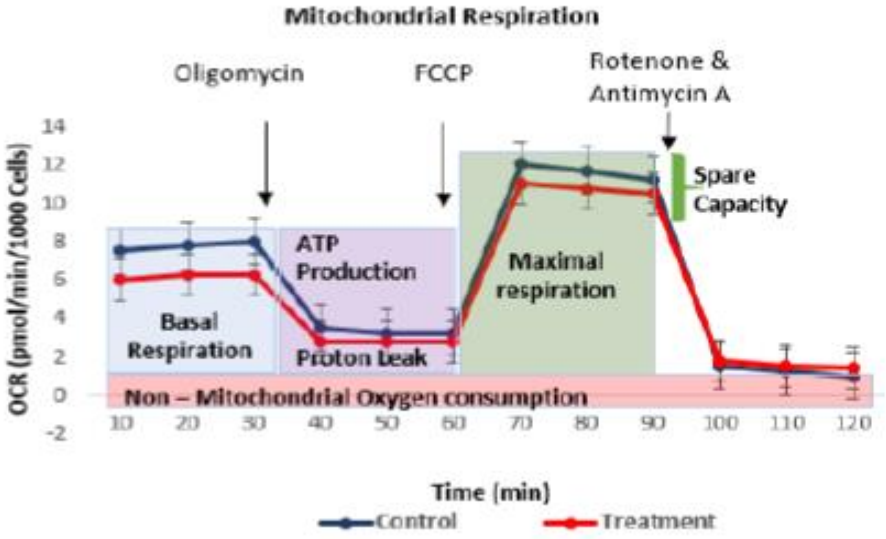

D.

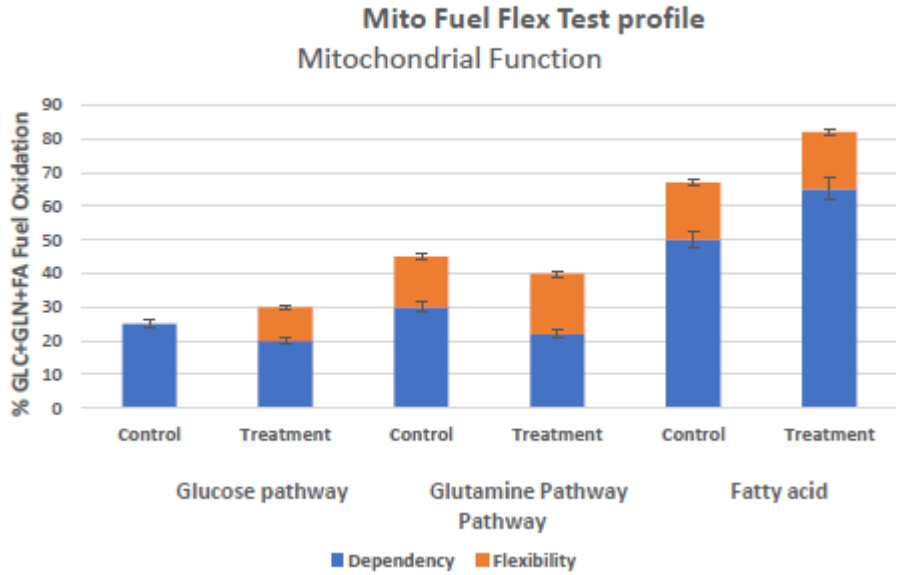

Click here to access/download

Table of Materials

MS Table of Materials.xls

VANDERBILT UNIVERSITY School of Medicine *Division of Clinical Pharmacology*

24 November 2021

Dear Dr. Krishnan,

We would ask that you reconsider our manuscript, entitled "**Using Seahorse XFe Analyzer to Monitor Osteoblast Bioenergetics**", for publication (JoVE63142). The original submission was received with enthusiasm, however, the reviewers constructively noted weaknesses. We thank the entire review team for all their valuable comments and suggestions that have significantly strengthened the manuscript.

To perform that revision, we started by directly addressing the specific weaknesses noted by the reviewers. This included:

(i) Grammatical and editorial reformatting of the entire manuscript.
(ii) The inclusion of additional experiment details, to include figures.
(iii) Refined 'Discussion'

This current resubmission represents our best and exhaustive efforts to address all the weaknesses noted and incorporate the reviewers' thoughtful suggestions. Additionally, this current version of the manuscript has been reformatted to adhere to the *JoVE* policies for data presentation and analyses. Please also find our line-by-line rebuttal on the following pages with our responses in *italics*.

Again, we wish to express our appreciation to you and the *JoVE* staff for consideration of our revised manuscript for publication.

Sincerely,

Elizabeth Rendina-Ruedy, Ph.D.
Assistant Professor of Medicine
Vanderbilt Center for Bone Biology
Division of Clinical Pharmacology
Department of Medicine
Vanderbilt University Medical Center

Assistant Professor

2200 Pierce Avenue
536 Robinson Research Building
Nashville, Tennessee 37232-6602

www.mc.vanderbilt.edu/clinicalpharmacology
tel 615.875.3049
fax 615.875.3297

Molecular Physiology and Biophysics
Vanderbilt University

2215b Garland Avenue
1155C MRBIV-Light Hall
Nashville, TN 37232
(615)-875-5247

DETAILED RESPONSE TO REVIEWERS*:*

Response: Please find below comments from the reviewers, along with our response in *italics*.

Reviewer #1:

Major Concerns:
1. Protocol, line 152: 48h incubation is suggested before the removal of non-attached cells. Previous works indicate that such a prolonged incubation results in presence of BMSC population heavily contaminated with hematopoietic cells. Shorter incubation is preferable given that BMSCs attach within the first 3 h.

Response: *Thank you for the comment. We recognize that some lab-to-lab variation exists in this step. In our hands, this specific protocol is followed. We have performed serial timepoints and quantification previously to determine 48 hours does not result in profound 'contamination' of HSCs, however, going past this timepoint does. It is true that we have also used 24 hr, therefore, we have edited the protocol to indicate this expanded timeframe. Again, in our experience HSCs generally stay as suspension in the media. While it is possible that some HSCs adhere to the plastic, they are not readily trypsin-sensitive and require scrapping, which we do not do. Prior to trypsinization we wash the cells thoroughly with PBS to get rid of the loosely adhered cells, thus further avoiding HSC contamination. There are several previously published reports as well referring to this [1, 2], along with even longer attachment incubations times [3-5].*
2. Line 237: 10mM Glucose is supraphysiological and comparable to diabetic levels. While 10 mM may be beneficial for cell growth and expansion, it may cause artifacts in assessing energy metabolism because of the possibility of the Crabtree effect, etc. Physiological 5 mM glucose is more appropriate
Response: *Thank you for this astute comment. We absolutely agree and appreciate the 'artificial' nature of Seahorse assays, even, 'normal' in vitro culturing systems. In this context, we have followed the manufacturer's recommended protocol of 10 mM glucose for these Seahorse assays, for ease of describing the assay. As we note multiple times, all substrates added to the Seahorse assay media can be altered, depending on the research question and study design. Therefore, we wanted to provide a general protocol, recognizing it can be altered. Additionally, other cells types have reported that this concentration to be ideal for measuring metabolic activity of mammalian cells [6]. Another study which has used different concentrations of glucose in media*

to measure OCAR and ECAR have shown increasing the glucose concentration from 5 to 10mM does not have any effect [7]. However, we have emphasized this point within the manuscript text and note its importance.

Minor Concerns:
1. Intro, line 48: incomplete sentence "Differentiation…"
Response: *Thank you for pointing out this mistake. We have corrected the sentence now. It now reads "Ex vivo/ in vitro differentiation of bone marrow stromal stem cells (BMSCs) to osteoblast precursors and mature osteoblasts results in the formation and deposition of bone mineralized bone matrix with the culture vessel over time." This is now Intro, line 49-52.*
2. Intro, line 65: correct "mitochondrial" for "mitochondria"
Response: Thank you for pointing out this mistake. We have corrected it from "mitochondrial" to "mitochondria". This is now Intro, line 69.

Reviewer #2:
Manuscript Summary:
This article describe a protocole for analyzing energy metabolism using Seahorse XFe Analyzer.
Major Concerns:
While this subject is interesting, there are many confusions in energy metabolism and misinterpretations of the various analytical parameters that render this protocol unusable in daily practice.
Response: *We appreciate your comments and taking the time to read through our manuscript. While we respectfully disagree with the comment related to 'unusable in daily practice', we have tried to address your concerns. To this end we use this current protocol daily, yielding high quality, repeatable, and publishable data. As we have noted, it is not possible to simply describe a universal protocol which will fit every lab and every research question. Similarly, it is not possible to provide all potential assays/ applications of the Seahorse analyzer. We have done our best to pick one and describe it sufficiently. Researchers must consider their individual experiences and scientific questions. The fundamentals of the assay remain constant, the Seahorse analyzer measures oxygen (O_2) and pH, has ability to alter metabolic exogenous substrates, and possibility of 4 injections. Therefore, many possible combinations exist, with the company providing the basics for defined assays.*

Reviewer #3:
Manuscript Summary:
Jayapalan et. al showed a detailed method of Using Seahorse XFe Analyzer to Monitor Osteoblast Bioenergetics in this manuscript. Protocol described in a detailed step by step manner. This article will be helpful to analyze cellular bioenergetics of osteoblast. However, I have few comments that authors need to address;

Minor Concerns:
1. For hydration of the sensor cartridge author used water, whereas agilent recommend specific calibrant solution. Provide reason for not using agilent recommended calibrant solution.

Response: *The company has recently updated this step (2018). As the reviewer points out, it was previously recommended to use the calibrant solution throughout this hydration step, more*

recently this has been changed. Accordingly, water is used for pre-wetting the plate the day prior to the assay as suggested by the manufacturer protocol. On the day of the assay, this water is replaced with pre-warmed calibrant solution 45-60 min prior to loading the injection ports of the sensor cartridge and incubated at 37°C in non-CO_2 incubator.

2. Figure 2, Highlighted well numbers are not in a perfect position, "A12" should be placed on the actual A12 well to avoid confusion.

Response: *Thank you for bringing this to our attention. We have now corrected this.*

3. Author should show representative cellular images acquired for normalization by Cytation 5 Imaging reader.

Response: *We appreciate this suggestion and have now included these images in Figure 5.*

References

[1] D.E. Maridas, E. Rendina-Ruedy, P.T. Le, C.J. Rosen, Isolation, Culture, and Differentiation of Bone Marrow Stromal Cells and Osteoclast Progenitors from Mice, J Vis Exp (131) (2018).

[2] S. Nadri, M. Soleimani, R.H. Hosseni, M. Massumi, A. Atashi, R. Izadpanah, An efficient method for isolation of murine bone marrow mesenchymal stem cells, Int J Dev Biol 51(8) (2007) 723-9.

[3] S. Sun, Z. Guo, X. Xiao, B. Liu, X. Liu, P.H. Tang, N. Mao, Isolation of mouse marrow mesenchymal progenitors by a novel and reliable method, Stem Cells 21(5) (2003) 527-35.

[4] P. Sreejit, K.B. Dilip, R.S. Verma, Generation of mesenchymal stem cell lines from murine bone marrow, Cell Tissue Res 350(1) (2012) 55-68.

[5] S. Huang, L. Xu, Y. Sun, T. Wu, K. Wang, G. Li, An improved protocol for isolation and culture of mesenchymal stem cells from mouse bone marrow, J Orthop Translat 3(1) (2015) 26-33.

[6] S. Lev, C. Li, D. Desmarini, D. Liuwantara, T.C. Sorrell, W.J. Hawthorne, J.T. Djordjevic, Monitoring Glycolysis and Respiration Highlights Metabolic Inflexibility of Cryptococcus neoformans, Pathogens 9(9) (2020).

[7] N. Jones, J. Piasecka, A.H. Bryant, R.H. Jones, D.O. Skibinski, N.J. Francis, C.A. Thornton, Bioenergetic analysis of human peripheral blood mononuclear cells, Clin Exp Immunol 182(1) (2015) 69-80.